Two-step strategy for improving the tribological performance of Si_3N_4 ceramics: controlled addition of SiC nanoparticles and graphene-based nanostructures

Javier Llorente, Cristina Ramírez, Manuel Belmonte*

Institute of Ceramics and Glass (ICV-CSIC), c/Kelsen 5, 28049 Madrid, Spain

Abstract

The tribological behaviour of silicon nitride (Si_3N_4) ceramics is investigated using a two-step strategy. A set of ceramic composites containing silicon carbide nanoparticles (SiC_n) is developed and, subsequently, graphene-based fillers are added to the Si_3N_4/SiC composite with the best tribological performance. The friction coefficient and wear rate of Si_3N_4 are reduced up to 22% and 40%, respectively, when a 10 vol.% of SiC_n is incorporated into the ceramic matrix due to its improved mechanical response. Si_3N_4/SiC composites containing 11 vol.% of graphene nanoplatelets (GNPs) or reduced graphene oxide sheets (rGOs) are analysed under isooctane lubrication and dry testing. rGOs composite leads to an important decrease of the friction coefficient (50%) under lubricated conditions, and an enhancement of the wear resistance (44%) under dry sliding tests, as compared to the reference Si_3N_4/SiC. The best performance of rGOs composite is due to the nature of the lubricating tribofilm and its excellent toughness.

Keywords: Tribology; friction; wear; ceramic composites; graphene

* Corresponding author. Phone: +34-917355863; Fax: +34-917355843. E-mail: mbelmonte@icv.csic.es (M. Belmonte)

1. Introduction

Non-oxide ceramics such as Si_3N_4 and SiC are commonly used for structural applications operating under highly demanding conditions, such as elevated temperature, friction and wear processes, and large mechanical loadings [1-3]. While Si_3N_4 stands out due to its good fracture toughness and strength responses, as well as to its significant wear resistance [4], SiC exhibits excellent thermal conductivity, higher hardness and better strength at high temperatures than Si_3N_4 [5]. To take advantage of these properties, the development of Si_3N_4/SiC composites with improved mechanical properties has extensively been investigated [6-14]. In general, the addition of SiC enhances the high temperature performance of Si_3N_4 ceramics and increases their hardness. With respect to the tribological properties of Si_3N_4/SiC composites, scarce works, most of them under dry testing conditions, have been reported [15-18], which showed distinct results. In this way, Gomes et al. [15] found that the addition of 10 wt.% SiC platelets or 5 wt.% SiC_n to a Si_3N_4 matrix did not improve its wear resistance under a severe wear regime, although the platelets reduced the friction coefficient of the reference material. Tatarko et al. [16, 17] observed that the presence of 5 vol.% of intergranular SiC particles decreased both the friction coefficient and the specific wear rate of Si_3N_4 ceramics independently of the rare-earth oxide employed as sintering additives and the temperature conditions of the tests. Finally, Shin et al. [18] also reported better tribological performance of composites containing up to 30 wt.% of SiC_n, reaching the best results for the material with 20 wt.% due to the combination of the improved hardness and fracture toughness attained for this material.

On the other hand, graphene-based nanostructures have strongly emerged as fillers able to substantially enhance the tribological properties of ceramics [19]. These 2D carbon nanostructures would allow the formation of a lubricant carbon-rich tribolayer on the

mated surfaces that could also protect against wear and, in addition, they increase the toughness of the ceramic composites which might reduce their wear by the surface fatigue mechanism during severe wear regimes. At present, there are several studies that analysed the tribological performance of Si_3N_4 and SiC composites containing graphene fillers under dry or lubricated (water or isooctane) testing conditions [20]. All of them reported a better wear behaviour for ceramic composites than for monolithic materials, with improvements in the wear resistance that scanned from 35% up to few orders of magnitude, data that depended on the filler content, the microstructural characteristics of the materials and the testing parameters. The friction coefficient also decreased with the addition of graphene, although to a lesser extent, with friction reductions typically in the range of 10 to 50%.

Taking into account the above results, a next logical step would be to join the capabilities of graphene-based fillers with those of Si_3N_4/SiC composites. However, to the best of our knowledge, there are no reports that explore this combination and, hence, the aim of this work is to investigate if graphene nanostructures can enhance the tribological performance of already superior ceramic composites such as Si_3N_4/SiC ones. This study has been first started with a preliminary work looking for the best reference material in terms of friction and wear under isooctane lubrication. These testing conditions look for potential automotive applications [21]. A set of ceramics has been processed by modifying the α/β ratio of the Si_3N_4 crystalline phases and the SiC content (10 and 40 vol.%), which would affect to the hardness and toughness. In a second stage, the tribological response of graphene fillers containing Si_3N_4/SiC composites has been extensively analysed. For this purpose, two different graphene-based nanostructures have been selected; in particular, graphene nanoplatelets (GNPs) and graphene oxides (GOs).

2. Experimental

2.1. Materials fabrication

First of all, a set of Si_3N_4 ceramics and Si_3N_4/SiC composites was processed. The Si_3N_4 starting powder composition was formed by Si_3N_4 (SN-E10, UBE Industries), Al_2O_3 (SM8, Baikowski Chimie) and Y_2O_3 (Grade C, H. C. Starck) with a weight ratio of 93:2:5, respectively, which were ball milled in ethanol for 24 h. The solvent was removed in a rotary evaporator and the dried powders were sieved through a 63 μm mesh. Si_3N_4/SiC compositions were prepared by replacing 10 and 40 wt.% of the Si_3N_4 composition by nano-β-SiC (Nanostructured & Amorphous Materials Inc. with mean particle size of ~50 nm) and using the above mixing procedure. The distinct powder compositions were spark plasma sintered (SPS, SPS-510CE, Fuji Electronic Industrial Co., Ltd.) at two different maximum temperatures (T_{max}) to develop materials with ~30% (T_{max} = 1600 ºC) and almost zero (T_{max} = 1700 ºC) of α-Si_3N_4 phase content. All the SPS tests were carried out under a vacuum atmosphere of ~6 Pa, applying a uniaxial pressure of 50 MPa during the heating cycle. T_{max} was hold for 5 min. Disc-shaped Si_3N_4 specimens (20 mm diameter and 3 mm thickness) were labelled as SN0 and SN30 according to the α-phase content; while Si_3N_4/SiC composites were identified as SNX-YSiC, where "X" and "Y" corresponded to the α-phase and SiC contents, respectively.

In the case of Si_3N_4/SiC/graphene composites, two graphene sources were selected: GNPs (N006-P, Angstron Materials Inc., lateral dimension ≤ 5 μm and thickness 10-20 nm) and GOs (N002-PDE, Angstron Materials Inc., lateral dimension ≤ 7 μm and thickness 2-3 nm). Graphene-based compositions were obtained by individually sonicating GNPs and GOs for 1 h in alcohol media. Then, each suspension was mixed and sonicated with the corresponding ceramic suspension previously prepared, as it was

detailed above. The amount of graphene fillers for the composites was 11 vol.%, which was selected as a compromise content between that necessary for achieving both the highest fracture toughness (4-8 vol.%) and the best tribological performance (20 vol.%) of Si_3N_4 and SiC ceramics [19, 22]. The SPS conditions of the composites were the same than for ceramic materials, except T_{max} that was fixed at 1620 ºC to achieve the full densification of the specimens as well as the required α-phase Si_3N_4 content (0 or 30%). Confocal micro-Raman spectroscopy (Alpha300 WITec GmbH) employing a laser excitation wavelength of 532 nm was used to check the crystallinity of the graphene nanostructures. GOs were in situ reduced to graphene (rGOs) during the SPS treatment, which was confirmed by an intensity ratio between D and G Raman bands (I_D/I_G) of 0.52. The composites were labelled as SNSiC/GNPs and SNSiC/rGOs, although in some figures the legends were simplified as GNPs and rGOs, respectively.

All the specimens reached densities, determined by the Archimedes' method, above 99.7% of the theoretical density (ρ_{th}) considering that ρ_{th} for Si_3N_4/SiC composites was 3.23 $g \cdot cm^{-3}$; while for SN/SiC/graphene ones was 3.13 $g \cdot cm^{-3}$. α/β-Si_3N_4 phase ratio was estimated by using X-ray diffractometry (XRD, Bruker D5000, Siemens) and Gazzara and Messier's method [23]. The analysis of the microstructure of the materials was carried out by scanning electron microscopy (SEM, Models TM1000 and S-4700, Hitachi) on polished and etched -plasma (CF_4/O_2) or basic (NaOH)- samples, as well as on fracture surfaces. The mean grain diameter (d_{50}) and aspect ratio (AR_{50}) of the ceramic materials were quantified by image analysis (ImageJ software) on SEM images, taking into account at least 500 features.

The elastic modulus (E) and hardness (H) were determined by depth sensing Vickers indentation at 49 N (Zhu 2.5, Zwick/Roell) on the surface perpendicular to the SPS pressing axis. Fracture toughness (K_{IC}) was assessed by two methods depending on the

type of material: i) Vickers indentation (IF) at 196 N using Miranzo and Moya's equation [24],in the case of ceramics, and ii) the surface crack in flexure method (SCF) for graphene-based composites and their corresponding equivalent reference ceramic material. In this case, a Knoop indentation at 100 N was performed at the centre of 14 mm x 2.2 mm x 1.8 mm bars. This method is detailed elsewhere [25]. The reason for using SCF instead IF is because graphene composites do not fully develop median/radial cracks with the latter technique, which avoids estimating K_{IC}. Mechanical data for all tests represent the average value of at least five well-defined measurements.

For the tribological characterization, a linear-reciprocating ball-on-plate configuration (Model UMT3, Bruker) was employed, where the balls were commercial Si_3N_4 spheres (Ø = 10.3 mm), and the plates corresponded to the manufactured materials that were polished to reach a surface roughness, R_a, below 0.15 µm. The tribological testing parameters were the following: stroke length of 2.5 mm, sliding frequency of 20 Hz, 360 m of sliding distance (l), room temperature, relative humidity below 20%, and applied load (F_N) that varied with the lubricating conditions. In this way, 50, 100, and 180 N were selected under isooctane lubrication (Merck, density and dynamic viscosity at 20 ºC of 0.692 g·cm^{-3} and 0.50 mPa·s, respectively) looking for simulating the working conditions of gasoline direct injection engines. In addition, the response of graphene composites was also investigated under dry sliding conditions and applying a load of 5 N. The friction coefficient (µ) was recorded during the sliding experiments, and the steady-state friction coefficient (μ_{ss}) was estimated considering the 200-360 m interval of the sliding distance. The wear volume of the plates (W_V) was assessed from the width and depth of the scars [22] employing a contact profilometer (Dektak XT, Bruker); whereas the wear rate (W_R) was calculated as $W_R = W_V/(F_N \cdot l)$. Tribological data correspond to the average value of a minimum of three consistent tests.

3. Results and discussion

3.1 Tribological behaviour of Si_3N_4/SiC composites

Figure 1 collects μ_{ss} and W_R data for all ceramics versus the applied load under isooctane lubrication. At first glance, it can be clearly observed that any material containing SiC decreased the friction coefficient compared to the monolithic Si_3N_4 ceramics, independently of the testing load (Figure 1a). The maximum reductions with the load in this tribological parameter varied from 22% at 50 N to 14% at 180 N. Besides, the α-Si_3N_4 phase content seems to have a negligible effect on the friction both in Si_3N_4 ceramics and Si_3N_4/SiC composites. Finally, the response of the whole set of Si_3N_4/SiC composites was quite homogenous and almost kept constant with the applied load.

Regarding the wear properties (Figure 1b), although all materials exhibited a mild wear response (~10^{-8} $mm^3 \cdot N^{-1} \cdot m^{-1}$), some differences can be extracted. In this way, the addition of large SiC contents (40 vol.%) had a negative impact on W_R as compared to the corresponding Si_3N_4 reference materials, particularly at loads below 180 N. In the case of composites with 10 vol.% of SiC, only those having a 30% of α-Si_3N_4 phase (SN30-10SiC) were able to substantially enhance the wear resistance of its equivalent reference material (SN30), decreasing W_R up to 29-40% with the applied load. This composite had also better wear behaviour than SN0, especially at 180 N with a 30% of reduction in W_R. The reason could be explained by the microstructural characteristics and mechanical properties of this composite (Table 1). In fact, SN30-10SiC presents a perfect combination of high E, H and K_{IC} values that would prevent of a microfracture controlled failure of the worn surfaces. Moreover, the Si_3N_4 grain size is one of the smallest of the set of materials (d_{50} = 0.42 μm) due to the grain refinement promoted by

SiC [13] and the limited α→β-phase transformation, which would reduce the wear volume due to particle pulled-out. Therefore, based on the excellent tribological properties of SN30-10SiC composite under isooctane lubrication, it has been selected as the reference matrix and filled with graphene nanostructures to explore if the tribological response can be further enhanced.

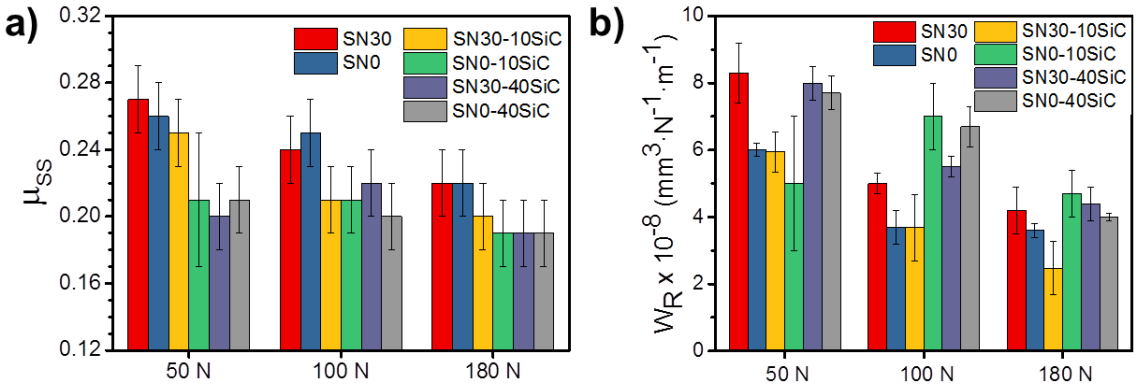

Figure 1. a) Steady-state friction coefficient (μ_{ss}) and b) wear rates (W_R) of Si_3N_4 ceramics and Si_3N_4/SiC composites as a function of the applied load tested under isooctane lubrication.

Table 1. Microstructural characteristics (d_{50} and AR_{50}) and mechanical properties (E, H and K_{IC}) for Si_3N_4 ceramics and Si_3N_4/SiC and Si_3N_4/SiC/graphene composites. K_{IC} data include the measurement method (IF or SCF).

Material	d_{50} (μm)	AR_{50} (μm)	E (GPa)	H (GPa)	K_{IC} (MPa·$m^{1/2}$)
SN30	0.52	1.9	313 ± 29	17.5 ± 0.5	5.6 ± 0.1 (IF)
SN0	1.20	2.3	288 ± 16	15.3 ± 0.5	6.2 ± 0.1 (IF)
SN30-10SiC	0.42	2.0	335 ± 11	19.0 ± 0.1	5.4 ± 0.2 (IF)

					5.1 ± 0.2 (SCF)
SN0-10SiC	0.62	2.2	312 ± 10	17.1 ± 0.2	5.5 ± 0.1 (IF)
SN30-40SiC	0.33	1.8	351 ± 41	19.5 ± 0.4	4.1 ± 0.5 (IF)
SN0-40SiC	0.62	2.0	330 ± 6	18.5 ± 0.1	5.0 ± 0.1 (IF)
SNSiC/GNPs	0.34	1.7	265 ± 22	10.8 ± 0.2	5.2 ± 0.2 (SCF)
SNSiC/rGOs	0.34	1.7	236 ± 7	9.0 ± 0.2	7.2 ± 0.4 (SCF)

3.2 Tribological behaviour of Si_3N_4/SiC/graphene composites

Figure 2 shows the microstructure of SN30-10SiC/GNPs and SN30-10SiC/rGOs composites, labelled as SNSiC/GNPs and SNSiC/rGOs, respectively, along their cross-sections. Both graphene fillers, especially rGOs, tend to align into the ceramic matrix with their basal plane perpendicular to the SPS pressing axis, which leads to anisotropic composites. The tribological properties were investigated in the specimen surface perpendicular to the SPS pressing axis (Figure 2); while the testing of the surface parallel to that axis has been dismissed because the arrangement of the fillers is less effective to promote both their pulling-out, limiting the lubrication capability, and an enhancement of the fracture toughness. Another important issue observed in the SEM images is that GNPs are shorter and thicker than rGOs (Figure 2a,c). The matrix characteristics are similar in both composites (Table 1), with a slight matrix grain refinement (d_{50} = 0.34 µm) as compared to the reference material (d_{50} = 0.42 µm), a well-known phenomenon produced by the addition of this type of fillers.

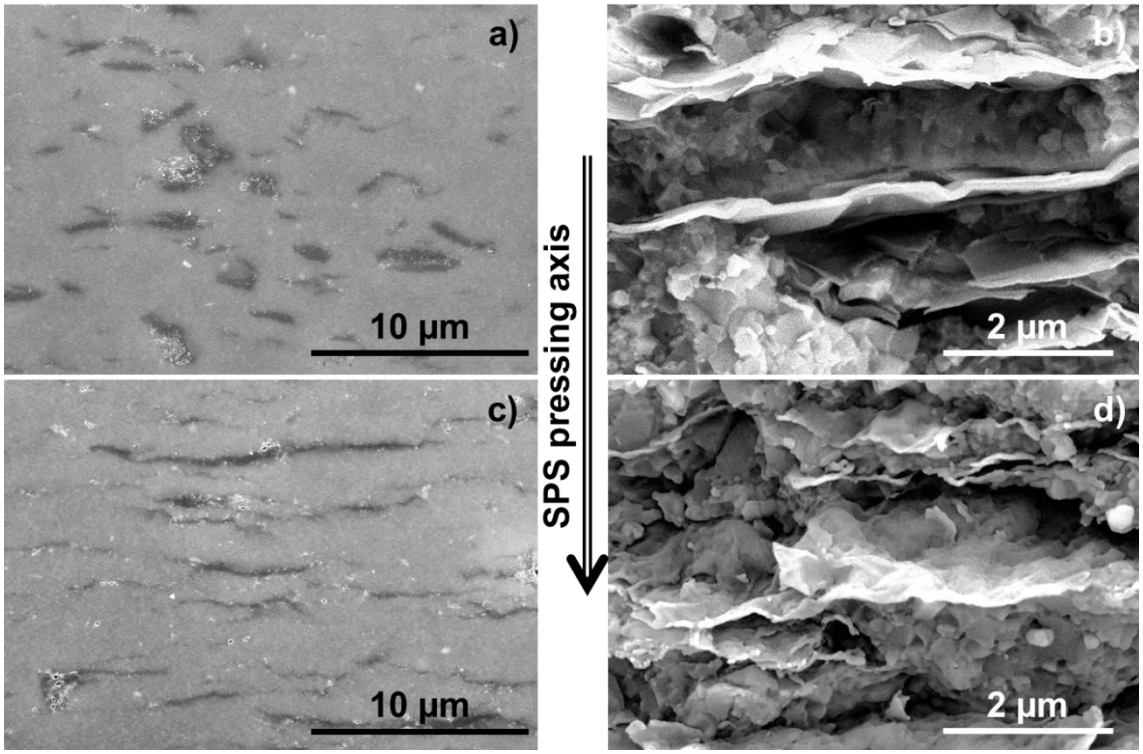

Figure 2. SEM images of the cross-section views corresponding to SNSiC/GNPs (a and b) and SNSiC/rGOs (c and d) composites. Images in the left column (a and c) were taken on polished specimens; while those shown in the right column (b and d) are fracture surfaces.

The friction response under isooctane lubrication evidenced a continuous decrease of μ_{ss} with the applied load (Figure 3a). Graphene fillers significantly reduced μ_{ss}, getting comparable values than those obtained for Si_3N_4/GNPs composites tested under identical tribological conditions [22]. Interestingly, that reduction is more pronounced for present rGOs-based composites. In this way, μ_{ss} diminished for this composite from 36% (at 50 N) to 50% (180 N) with respect to the reference material, which already presented an excellent friction behaviour within the set of distinct Si_3N_4 and Si_3N_4/SiC ceramics (Figure 1a). Regarding the wear resistance, similarly to the reference material, graphene-based composites also exhibited mild wear (Figure 3b), although the addition

of fillers had a detrimental effect on the wear performance. This negative impact is larger for GNPs than for rGOs as SNSiC/GNPs composite is the least wear resistant material within the whole range of applied loads. Compared to Si_3N_4/GNPs composites [22], current SNSiC/GNPs materials present slightly higher W_R values, although in the same order of magnitude (10^{-8} $mm^3 \cdot N^{-1} \cdot m^{-1}$), which could be explained by the smallest dimensions of the GNPs employed in Si_3N_4/GNPs composites that would reduce the material removal. The case of SNSiC/rGOs is slightly different because W_R decreased at low load (50 N) in about 22% as compared to the reference material, but as the load augmented the wear resistance of the reference material progressively enhanced.

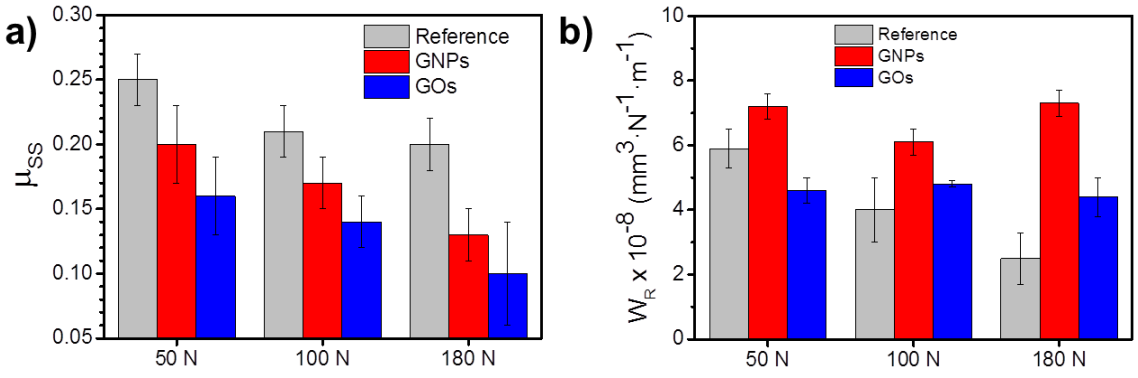

Figure 3. a) Steady-state friction coefficient (μ_{ss}) and b) wear rates (W_R) of SN30-10SiC ceramics (Reference) and SNSiC/GNPs (GNPs) and SNSiC/rGOs (rGOs) composites as a function of the applied load tested under isooctane lubrication.

Worn surfaces of the reference material and SNSiC/rGOs composite (Figure 4) showed the presence of a tribofilm that is more compacted and continuous as the applied load increased. This tribofilm would be formed by isooctane and debris particles coming from the counterparts [22] and, in the case of graphene-based composites, it would also include GNPs or rGOs pulled-out from the matrix and mechanically crushed that would act as solid lubricant, reducing the friction coefficient [22]. In addition, considering that

the wear rate in graphene composites hardly changed with the load (Figure 3b), it is possible to assume that once a certain degree of GNPs or rGOs was pulled-out, the removal of material was limited and the detached flakes were exfoliated as the load augmented, promoting the formation of a lubricating tribofilm. This process seems to be more effective when using rGOs instead of GNPs (Figure 3a), probably due to the large distribution of the rGOs within the material through a network that allows them actively acting in the formation of that tribofilm.

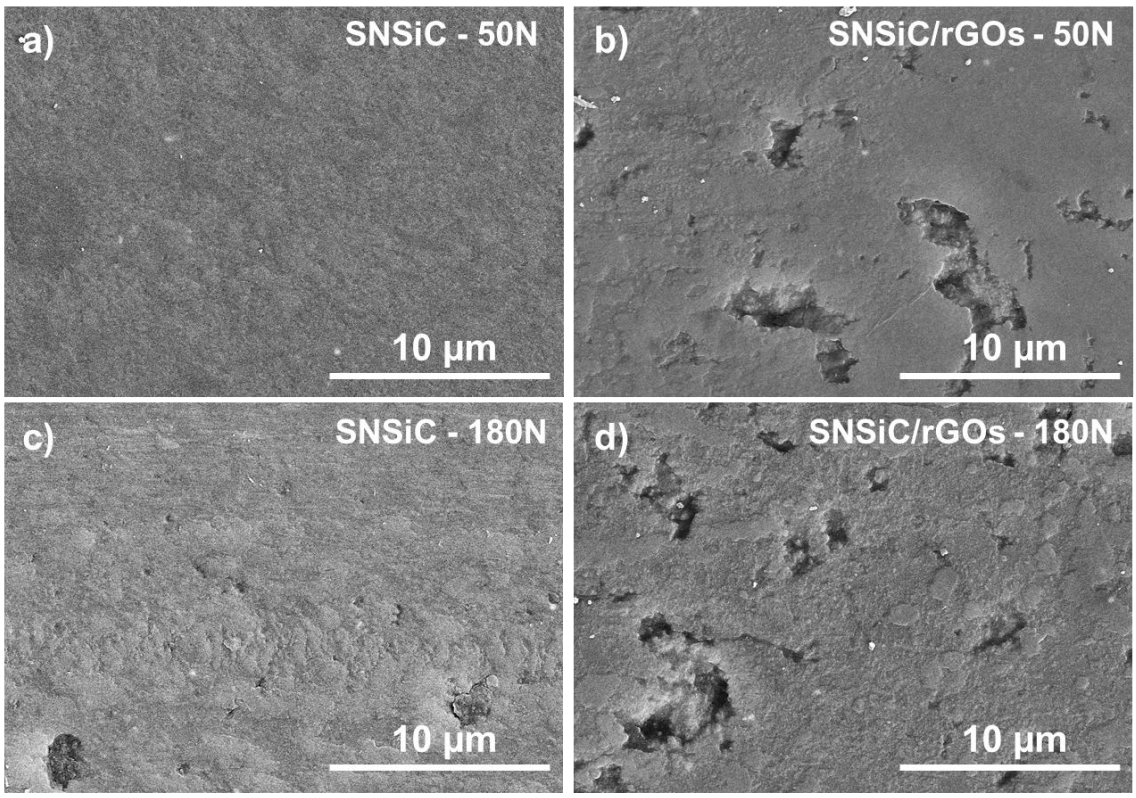

Figure 4. SEM micrographs of SNSiC (a and c) and SNSiC/rGOs (b and d) tracks after the tests performed under isooctane lubrication at 50 N (a and b) and 180 N (c and d).

Tribosystems working under a mild wear regime can exhibit distinct relationships between W_R and some mechanical parameters. Here, we have considered the model

proposed by Adachi et al. [26], which establishes that an augment of the wear rate has a linear dependence with the severity index parameter (S_{CM}):

$$S_{CM} = \frac{(1+10\,\mu_{ss})P_0\sqrt{R_Z}}{K_{IC}} \quad (1)$$

being P_0 the maximum Hertzian contact pressure and R_z a roughness parameter. This dimensionless index has, thus, a direct dependence with the friction behaviour through μ_{ss} and with E, as it takes part in P_0 estimation, and it has also an inverse relationship with K_{IC}. In the current composites, only SNSiC/rGOs is able to improve the toughness of the reference material, in particular about 41% (Table 1), due to the occurrence of numerous crack shielding mechanisms [25]. This is not the case for GNPs composites. The reason can be explained because, in general, the highest K_{IC} improvements are achieved for GNPs and rGOs contents much lower than 11 vol.% [25]. As the amount of fillers augments, the mechanical enhancement decreases faster for GNPs than for rGOs, which is a consequence of the formation of a thick graphene stacks network that decreases the effectiveness of the toughening mechanisms. When plotting W_R versus S_{CM} (Figure 5), an excellent correlation of the experimental data to the fittings was observed at intermediate and high loads; being less accurate at low load. Therefore, the wear behaviour depends on a cocktail formed by the surface and mechanical parameters where μ_{ss} and K_{IC} play a paramount role.

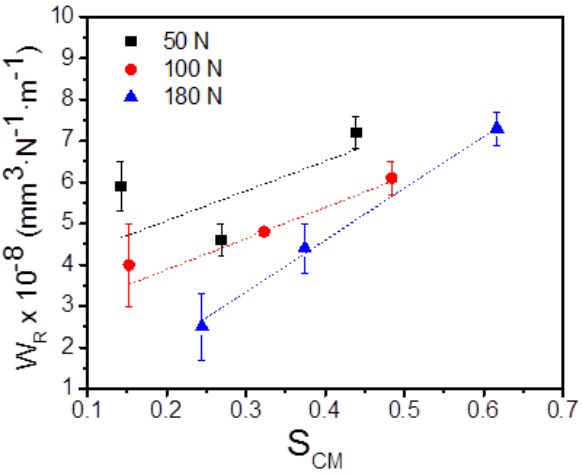

Figure 5. W_R versus S_{CM} for SNSiC ceramics and SNSiC/graphene composites as a function of the applied load of tests performed under isooctane lubrication.

SNSiC ceramics and SNSiC/graphene composites were also tested using dry sliding conditions. All of them presented a similar friction coefficient (~0.55) in the steady state region (Figure 6a), needing a running-in period of about 120 m of sliding distance to reach a stable behaviour, which occurs at slightly higher μ values for GNPs-based composites than for the rest of materials. Hence, the addition of graphene-based nanostructures seems to have a negligible effect on the friction response under these testing conditions. This is quite consistent with the results reported by the present authors when investigated dense SiC/graphene composites employing the same tribological parameters [27]. Regarding the wear response (Figure 6b), all tested materials evidenced a severe wear, in agreement with their W_R exponents (-5). However, while GNPs led to identical W_R values than the reference material, rGOs fillers promoted a significant reduction in this parameter of ~44%.

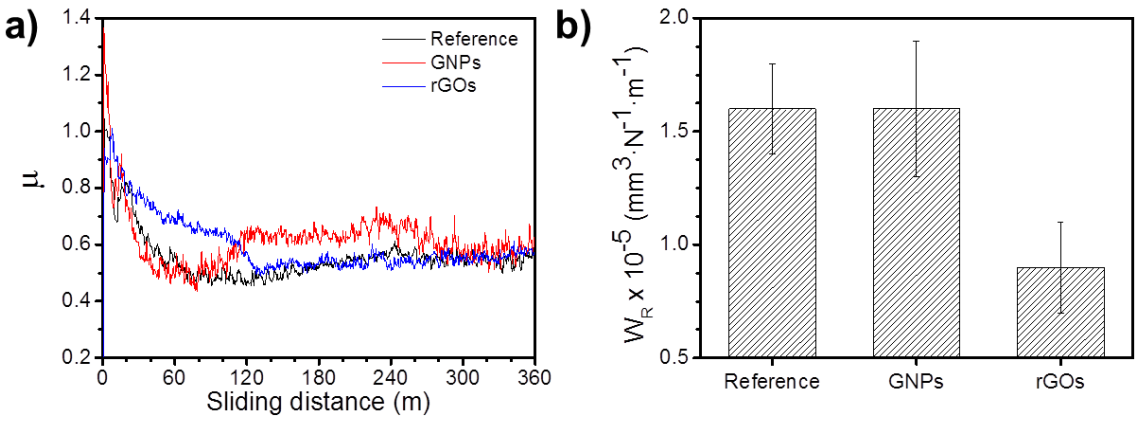

Figure 6. a) Average friction coefficient (μ) dynamic evolution considering three valid tests and b) wear rate (W_R) of SN30-10SiC ceramics (Reference) and SNSiC/GNPs (GNPs) and SNSiC/rGOs (rGOs) composites tested under dry conditions.

Figure 7 collects some SEM images of the worn surfaces after the dry sliding tests. As it can be seen, the wear track for the reference ceramics presents some rolls on a smooth surface (Figure 7a). These rolls, based on silicon hydroxide or silica, would be formed by means of tribochemical reactions between non-oxide ceramics and water molecules coming from the humidity in the environment [28]. In the case of SNSiC/rGOs composite, the appearance of the worn surface is quite different (Figure 7b), showing a large number of debris, a mixture of small rounded particles and elongated rolls, on a compacted dense tribolayer that fully covers the tribocontact. These rolls can be of the same nature than the reference material but the formation of graphene-based rolls coming from the detached rGO flakes cannot be discarded, as it has been recently observed by present authors in cubic yttria-stabilized zirconia/GNPs composites [29]. The wear track for SNSiC/GNPs presented very few rolls on a compacted rough tribofilm (Figure 7c), being a situation intermediate between those of the other two materials. Therefore, one of the reasons for the better wear performance of rGOs-based

composites could be explained by a most effective roller bearing-like effect that would partially redistribute the load at the tribocontact.

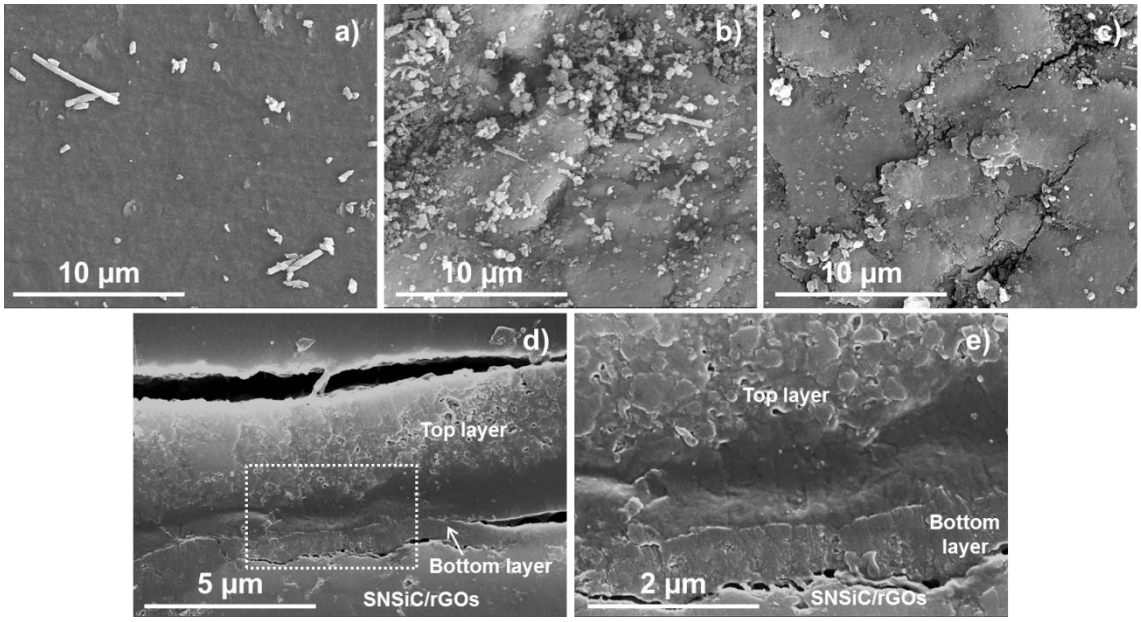

Figure 7. SEM micrographs of the worn surfaces after the tests performed under dry conditions for: a) the reference material, b) SNSiC/rGOs and c) SNSiC/GNPs composites. d) Image of the cross-section of the tribofilm formed in the SNSiC/rGOs surface and e) high magnification of the area enclosed into the dashed window in d) showing the tribofilm formed by a double layer.

The compacted tribolfilms in both graphene composites were formed by ceramic- and carbon-based debris, the latter confirmed by Raman microscopy. In fact, I_D/I_G of the SNSiC/GNPs surface varied from 0.13 (untested) to 1.06 (wear track); while for SNSiC/rGOs changed from 0.52 (untested) to 0.95 (wear track). These values would confirm that graphene nanostructures (GNPs and rGOs) on the tested surface were damaged during the tribotests and, consequently, the D-band intensity linked to defects augmented. A close examination of the cross-section of the tribofilm formed on the SNSiC/rGOs specimen revealed a structure of double layer (Figures 7d,e): a bottom thin layer of about ~1 µm thickness joined to the pristine material and a thicker top layer (~

4 μm) with larger grain size. The bottom one would increase the mechanical resistance of the whole tribofilm due to its smaller grain size that would act as an anchorage layer. This layer would be created during the initial stages of the wear process, and it is formed by highly compacted small debris that were mechanically crushed during the sliding motion due to high Hertzian pressures; while in the top layer, debris appeared compacted but less smashed (Figure 7e). This kind of double layer has been previously mentioned in non-asbestos organic brakes filled with carbon nanotubes and zirconia nanoparticles [30], the present work being the first, to the best of our knowledge, which reports the formation of a tribofilm based on a double layer in ceramic/graphene composites.

Surface fatigue, and the corresponding microcracks formation beneath the contact, is one of the most common wear mechanisms that take place under a severe wear regime and, thus, the fracture toughness is an essential parameter to enhance the wear performance. If W_R is plotted against K_{IC} for the different materials (Figure 8), a consistent dependence between both parameters can be observed. In this way, the materials with the worst fracture toughness performances -reference ceramics and SNSiC/GNPs composites- also exhibited the lowest wear resistances. Conversely, SNSiC/rGOs composite, with the highest K_{IC} value (7.2 MPa·$m^{1/2}$, a 41% higher than the reference material) improved the wear response in about 44% as compared with the other materials.

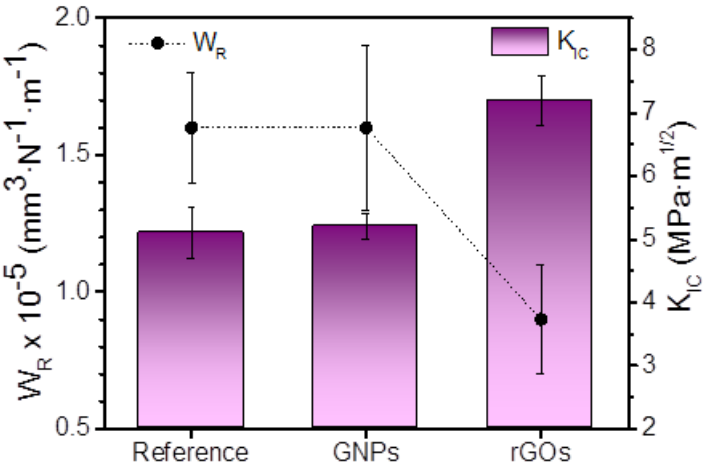

Figure 8. W_R under dry sliding conditions and K_{IC} for SNSiC ceramic and SNSiC/graphene composites.

There are scarce works devoted to the comparison of the wear properties of ceramic composites under dry conditions using graphene fillers with different thickness [27, 31]. In these works, it seems that for SiC or Si_3N_4 ceramics containing ~5 vol.% of graphene, thinner fillers -rGOs [27] or exfoliated GNPs [31]- slightly improved (9-14%) the wear resistance as compared to the equivalent composite filled by thicker graphene stacks (namely GNPs). That improvement would be linked to an enhanced filler dispersion of thin graphene flakes that increased the fracture toughness. In the present case, where fillers content is larger (11 vol.%), rGOs enlarged the benefits in the wear response (44%) with respect to GNPs due to a higher fracture toughness of the composite and, to a lesser extent, the roller bearing-like effect.

4. Conclusions

Si_3N_4 ceramics with a good tribological response under isooctane lubrication exhibit a clear improvement in their friction (up to 22%) and wear (up to 40%) behaviour by

adding 10 vol.% of SiC_n. This enhanced performance of Si_3N_4/SiC composites is a direct consequence of their high mechanical values (E, H and K_{IC}) that prevent of a microfracture controlled failure of the tested surfaces. The introduction of 11 vol.% of graphene-based fillers (GNPs or rGOs) into that ceramic composites leads to a significant reduction in the friction coefficient (up to 50%), which is especially favoured by rGOs because they promote a more effective development of a carbon-based lubricating tribofilm. However, the graphene nanostructures have a detrimental effect in the wear resistance of Si_3N_4/SiC composites, and only a better performance (22%) is observed at low loads when using rGOs. A direct correlation between the wear rate and the severity index of the tested materials is observed, with the friction and the fracture toughness playing a key role in the mild wear process.

GNPs and rGOs seem to have a negligible effect on the friction response of Si_3N_4/SiC composites under dry sliding conditions, although, conversely, rGOs allows significantly increasing (44%) the wear resistance of the reference material. The presence of rolls on top of a compacted double-layer tribofilm that would partially redistribute the load at the tribocontact, jointly with a 41% higher fracture toughness than the reference material would explain the best wear performance attained for rGOs composites.

The tribological performance of Si_3N_4 ceramics under isooctane lubricated and dry sliding conditions has been enhanced through a two-step strategy based on the progressive addition of SiC nanoparticles and rGOs fillers.

Acknowledgements

This work was supported by the Spanish project RTI2018-095052-BI00 (MCIU/AEI/FEDER, UE). C. R. acknowledges the support of Juan de la Cierva postdoctoral fellowship program.

References

[1] Z. Krstic, V. D. Krstic, Silicon nitride: the engineering material of the future, J. Mater. Sci. 47 (2012) 535-552. https://doi.org/10.1007/s10853-011-5942-5

[2] F. L. Riley, Silicon nitride and related materials, J. Am. Ceram. Soc. 83 (2000) 245-265. https://doi.org/10.1111/j.1151-2916.2000.tb01182.x

[3] K. A. Schwetz, Silicon carbide based hard materials, Handbook of Ceramic Hard Materials, WILEY-VCH Verlag GmbH, Weinheim, 2008. https://doi.org/10.1002/9783527618217.ch20

[4] M. H. Bocanegra-Bernal, B. Matovic, Mechanical properties of silicon nitride-based ceramic and its use in structural applications at high temperature, Mater. Sci. Eng. A 527 (2010) 1314-1338. https://doi.org/10.1016/j.msea.2009.09.064

[5] G. Roewer, U. Herzog, K. Trommer, E. Müller, S. Frühauf, Silicon carbide-a survey of synthetic approaches, properties and applications, High Perform. Non-Oxide Ceram.: I Struct. Bond. 101 (2002) 59-135.

[6] M. Sternitzke, Structural ceramic nanocomposites, J. Eur. Ceram. Soc. 17 (1997) 1061-1082. https://doi.org/10.1016/S0955-2219(96)00222-1

[7] P. Rendtel, A. Rendtel, H. Hübner, Mechanical properties of gas pressure sintered Si_3N_4/SiC nanocomposites, J. Eur. Ceram. Soc. 22 (2002) 2061-2070. https://doi.org/10.1016/S0955-2219(01)00526-X

[8] J. Wan, R.-G. Duan, M. J. Gasch, A. K. Mukherjee, Highly creep-resistant silicon nitride/silicon carbide nano-nano composites, J. Am. Ceram. Soc. 89 (2006) 274-280. https://doi.org/10.1111/j.1551-2916.2005.00702.x

[9] L. Hegedusova, M. Kasiarova, J. Dusza, M. Hnatko, P. Sajgalik, Mechanical properties of carbon-derived Si_3N_4+SiC micro/nano composite, Int. J. Refractory Metals 27 (2009) 438-442. https://doi.org/10.1016/j.ijrmhm.2008.09.012

[10] M. Balog, J. Keckes, T. Schöberl, D. Galusek, F. Hofer, J. Krestan, Z. Lences, J.-L. Huang, P. Sajgalik, Nano/macro-hardness and fracture resistance of Si_3N_4/SiC composites with up to 13 wt.% of SiC nano-particles, J. Eur. Ceram. Soc. 27 (2007) 2145-2152. https://doi.org/10.1016/j.jeurceramsoc.2006.08.010

[11] V. Biasini, S. Guicciardi, A. Bellosi, Silicon nitride-silicon carbide composite materials, Int. J. Refractory Metals 11 (1992) 213-221. https://doi.org/10.1016/0263-4368(92)90048-7

[12] T. Hirano, K. Niihara, Microstructure and mechanical properties of Si_3N_4/SiC composites, Mater. Lett. 22 (1995) 249-254. https://doi.org/10.1016/0167-577X(94)00255-X

[13] J.-F. Yang, T. Ohji, T. Sekino, C.-L. Li, K. Niihara, Phase transformation microstructure and mechanical properties of Si_3N_4/SiC composite, J. Eur. Ceram. Soc. 21 (2001) 2179-2183. https://doi.org/10.1016/S0955-2219(01)00193-5

[14] F. Eblagon, B. Ehrle, T. Graule, J. Kuebler, Development of silicon nitride/silicon carbide composites for wood-cutting tools, J. Eur. Ceram. Soc. 27 (2007) 419-428. https://doi.org/10.1016/j.jeurceramsoc.2006.02.040

[15] J. R. Gomes, M. I. Osendi, P. Miranzo, F. J. Oliveira, R. F. Silva, Tribological characteristics of self-mated couples of Si_3N_4-SiC composites in the range 22-700 ºC, Wear 233 (1999) 222-228. https://doi.org/10.1016/S0043-1648(99)00243-4

[16] P. Tatarko, M. Kasiarova, J. Dusza, J. Morgiel, P. Sajgalik, P. Hvizdos, Wear resistance of hot-pressed Si_3N_4/SiC micro/nanocomposites sintered with rare-earth oxide additives, Wear 269 (2010) 867-874. https://doi.org/10.1016/j.wear.2010.08.020

[17] P. Tatarko, M. Kasiarova, Z. Chlup, J. Dusza, P. Sajgalik, I. Vavra, Influence of rare-earth oxide additives and SiC nanoparticles on the wear behaviour of Si_3N_4-based composites at temperatures up to 900 ºC, Wear 300 (2013) 155-162. https://doi.org/10.1016/j.wear.2013.01.030

[18] J.-H. Shin, B. V. M. Kumar, J.-H. Kim, S.-H. Hong, Tribological properties of Si_3N_4/SiC nano-nano composite ceramics, J. Am. Ceram. Soc. 94 (2011) 3683-3685. https://doi.org/10.1111/j.1551-2916.2011.04847.x

[19] P. Miranzo, M. Belmonte, M. I. Osendi, From bulk to cellular structures: a review on ceramic/graphene filler composites, J. Eur. Ceram. Soc. 37 (2017) 3649-3672. https://doi.org/10.1016/j.jeurceramsoc.2017.03.016

[20] M. Belmonte, Contact damage, friction and wear response of ceramic composites, in Encycopledia of Materials:Technical Ceramics and Glasses. Ed. F. Cambier and A. Leriche, Elsevier, In Press. https://doi.org/10.1016/B978-0-12-818542-1.12134-4

[21] J. Kirwan, M. Shost, G. Roth, J. Zizelman, 3-Cylinder turbocharged of gasoline direct injection: a high value solution for low CO_2 and NO_x emissions, SAE Int. J. Engines 3 (2010) 355-371. https://www.jstor.org/stable/26275487

[22] J. Llorente, C. Ramírez, M. Belmonte, High graphene fillers content for improving the tribological performance of silicon nitride-based ceramics, Wear, 430-431 (2019) 183-190. https://doi.org/10.1016/j.wear.2019.05.004

[23] C. P. Gazzara, D. R. Messier, Determination of phase content of Si_3N_4 by X-Ray diffraction analysis, Am. Ceram. Soc. Bull. 56 (1977) 777-780.

[24] P. Miranzo, J. Moya, Elastic/plastic indentation in ceramics: a fracture toughness determination method, Ceram. Int. 10 (1984) 147-152. https://doi.org/10.1016/0272-8842(84)90005-1

[25] C. Ramírez, P. Miranzo, M. Belmonte, M. I. Osendi, P. Poza, S. Vega-Díaz, M. Terrones, Extraordinary toughening enhancement and flexural strength in Si_3N_4 composites using graphene sheets, J. Eur. Ceram. Soc. 34 (2014) 161-169. https://doi.org/10.1016/j.jeurceramsoc.2013.08.039

[26] K. Adachi, K. Kato, N. Chen, Wear map of ceramics, Wear 203 (1997) 291-301. https://doi.org/10.1016/S0043-1648(96)07363-2

[27] J. Llorente, B. Román-Manso, P. Miranzo, M. Belmonte, Tribological performance under dry sliding conditions of graphene/silicon carbide composites, J. Eur. Ceram. Soc. 36 (2016) 429-435. https://doi.org/10.1016/j.jeurceramsoc.2015.09.040

[28] H. Tomizawa, T. E. Fischer, Friction and wear of silicon nitride and silicon carbide in water: hydrodynamic lubrication at low sliding speed obtained by tribochemical wear, ASLE Trans. 30 (1987) 41-46. https://doi.org/10.1080/05698198708981728

[29] J. Llorente, M. Belmonte, Rolled and twisted graphene flakes as self-lubricant and wear protecting fillers into ceramic composites, Carbon 159 (2020) 45-50. https://doi.org/10.1016/j.carbon.2019.12.026

[30] Q. Che, H. Li, L. Zang, F. Zhao, G. Li, Y. Guo, J. Zhang, G. Zhang, Role of carbon nanotubes on growth of a nanostructured double-deck tribofilm yielding excellent self-lubrication performance, Carbon 161 (2020) 445-455. https://doi.org/10.1016/j.carbon.2020.01.091

[31] O. Tapaszto, J. Balko, V. Puchy, P. Kun, G. Dobrik, Z. Fogarassy, Z. E. Horvath, J. Dusza, K. Balazsi, C. Balazsi, L. Tapaszto, Highly wear-resistant and low friction Si_3N_4 composites by addition of graphene nanoplatelets approaching the 2D limit, Sci. Rep.7 (2017) 10087. https://doi.org/10.1038/s41598-017-10290-5

Table caption

Table 1. Microstructural characteristics (d_{50} and AR_{50}) and mechanical properties (E, H and K_{IC}) for Si_3N_4 ceramics and Si_3N_4/SiC and Si_3N_4/SiC/graphene composites. K_{IC} data include the measurement method (IF or SCF).

Table 1

Material	d_{50} (μm)	AR_{50} (μm)	E (GPa)	H (GPa)	K_{IC} ($MPa \cdot m^{1/2}$)
SN30	0.52	1.9	313 ± 29	17.5 ± 0.5	5.6 ± 0.1 (IF)
SN0	1.20	2.3	288 ± 16	15.3 ± 0.5	6.2 ± 0.1 (IF)
SN30-10SiC	0.42	2.0	335 ± 11	19.0 ± 0.1	5.4 ± 0.2 (IF) 5.1 ± 0.2 (SCF)
SN0-10SiC	0.62	2.2	312 ± 10	17.1 ± 0.2	5.5 ± 0.1 (IF)
SN30-40SiC	0.33	1.8	351 ± 41	19.5 ± 0.4	4.1 ± 0.5 (IF)
SN0-40SiC	0.62	2.0	330 ± 6	18.5 ± 0.1	5.0 ± 0.1 (IF)
SNSiC/GNPs	0.34	1.7	265 ± 22	10.8 ± 0.2	5.2 ± 0.2 (SCF)
SNSiC/rGOs	0.34	1.7	236 ± 7	9.0 ± 0.2	7.2 ± 0.4 (SCF)

Figure 1

Click here to download high resolution image

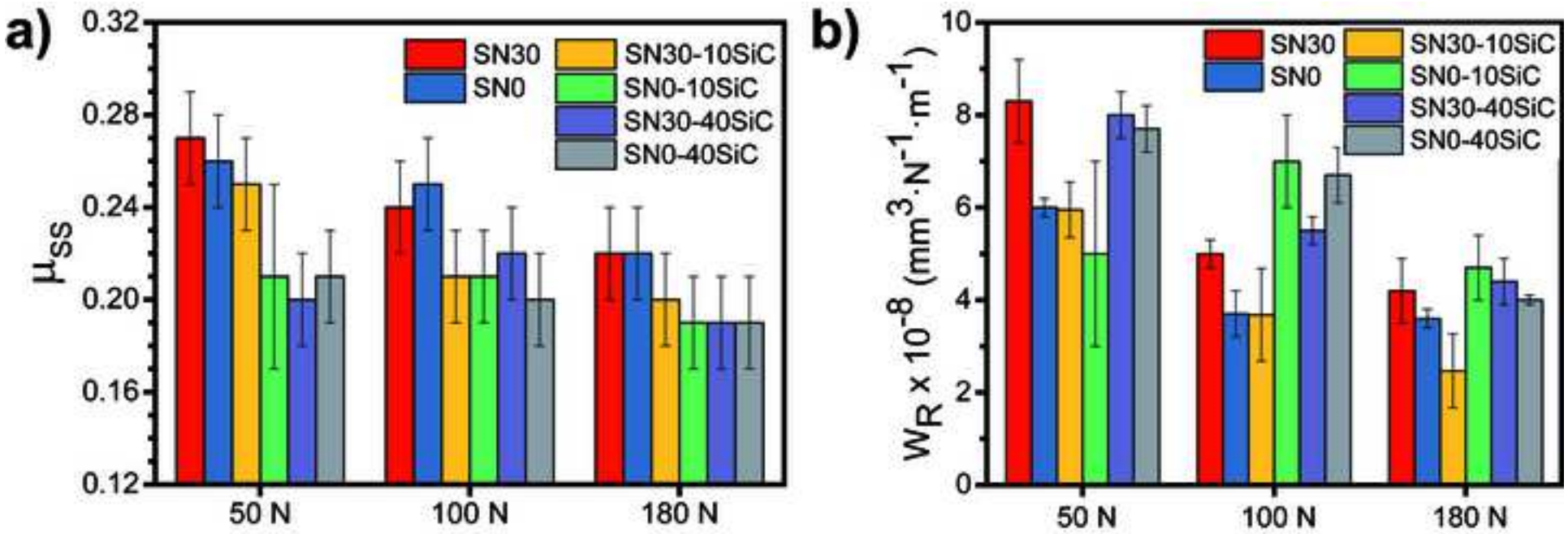

Figure 2
Click here to download high resolution image

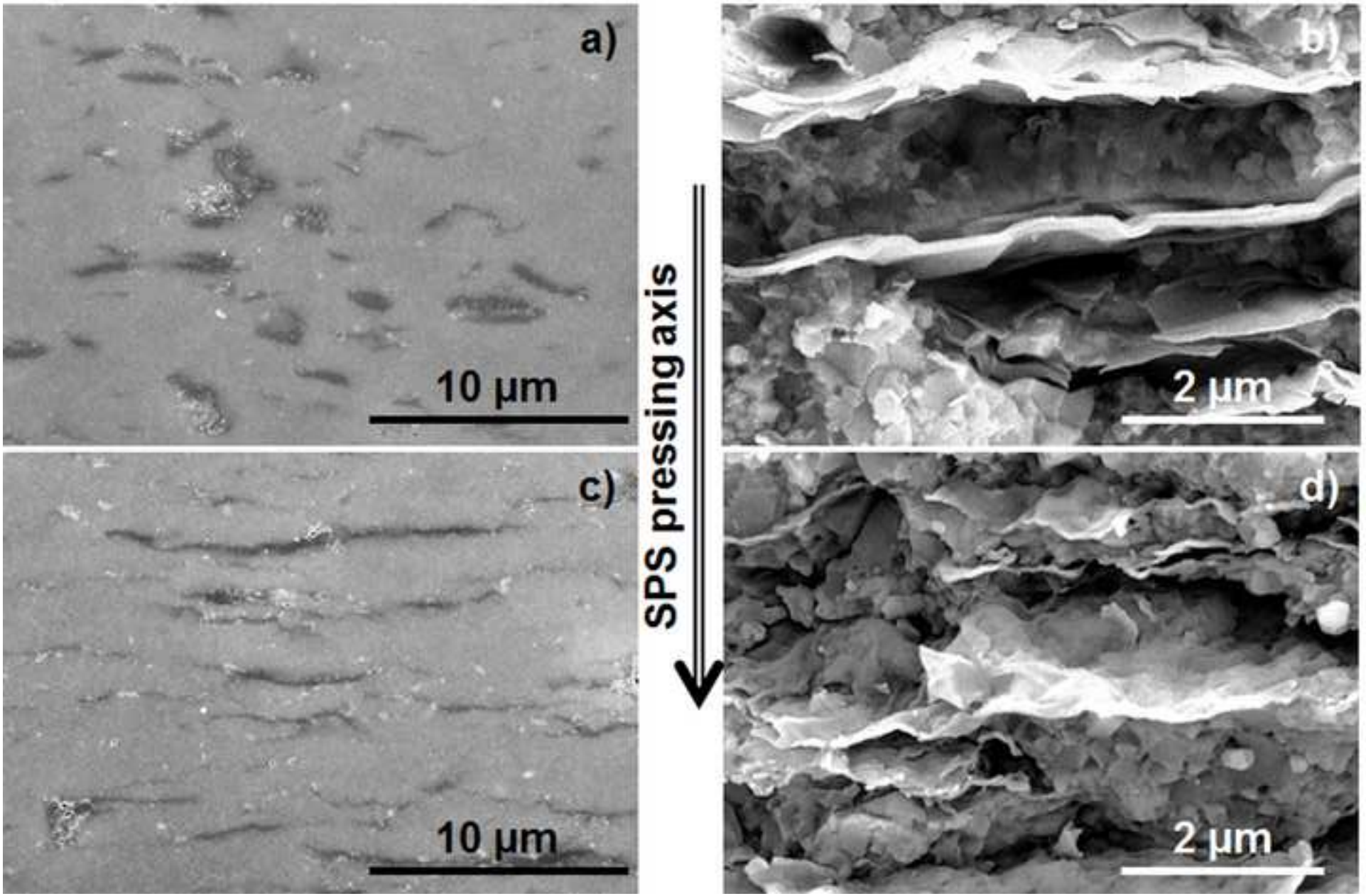

Figure 3

Click here to download high resolution image

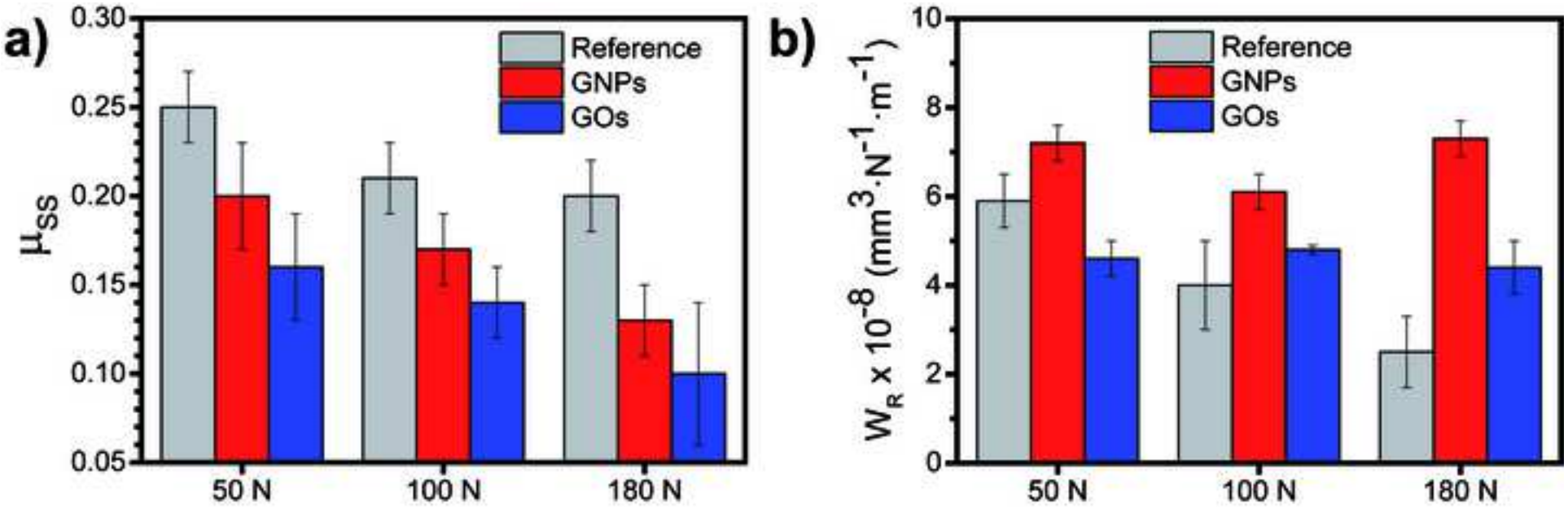

Figure 4
Click here to download high resolution image

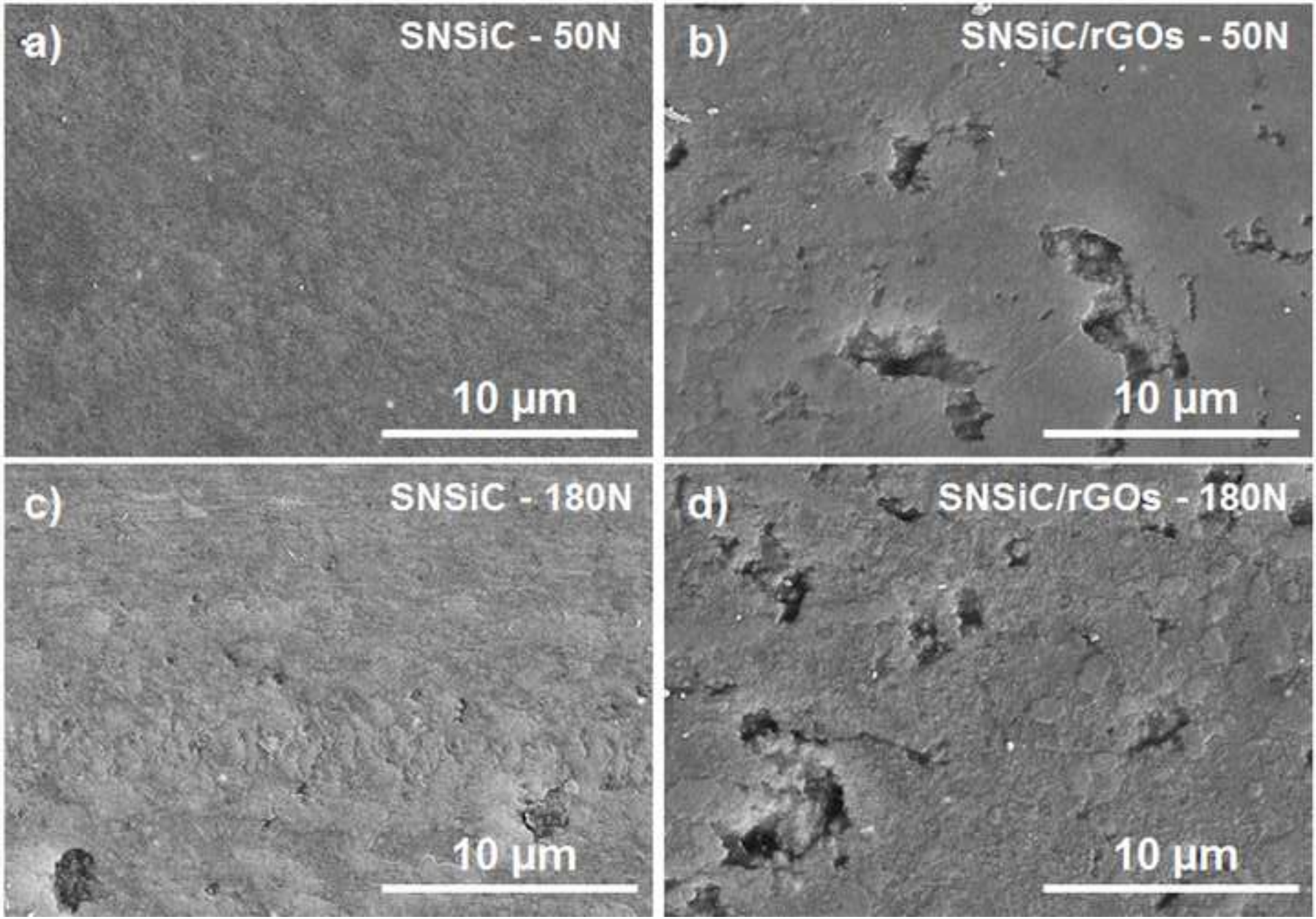

Figure 5

Click here to download high resolution image

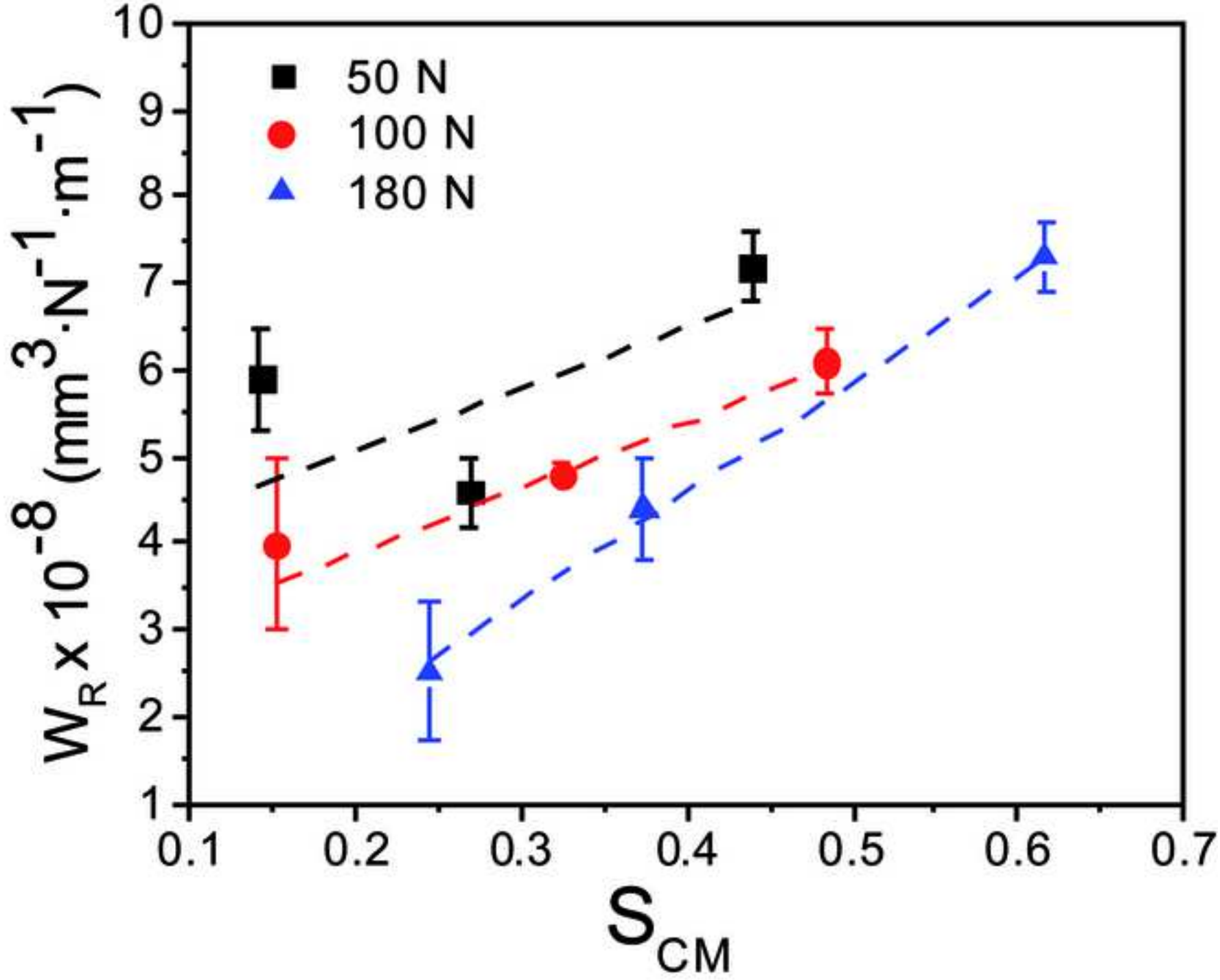

Figure 6

Click here to download high resolution image

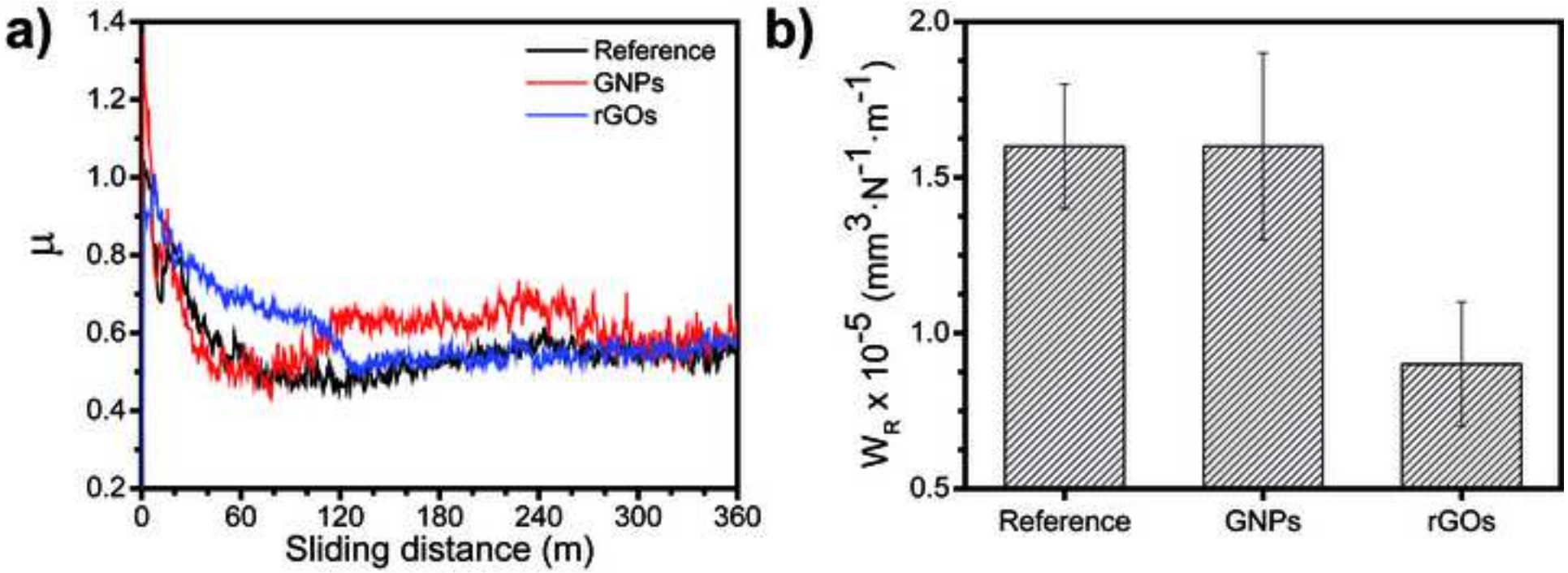

Figure 7

Click here to download high resolution image

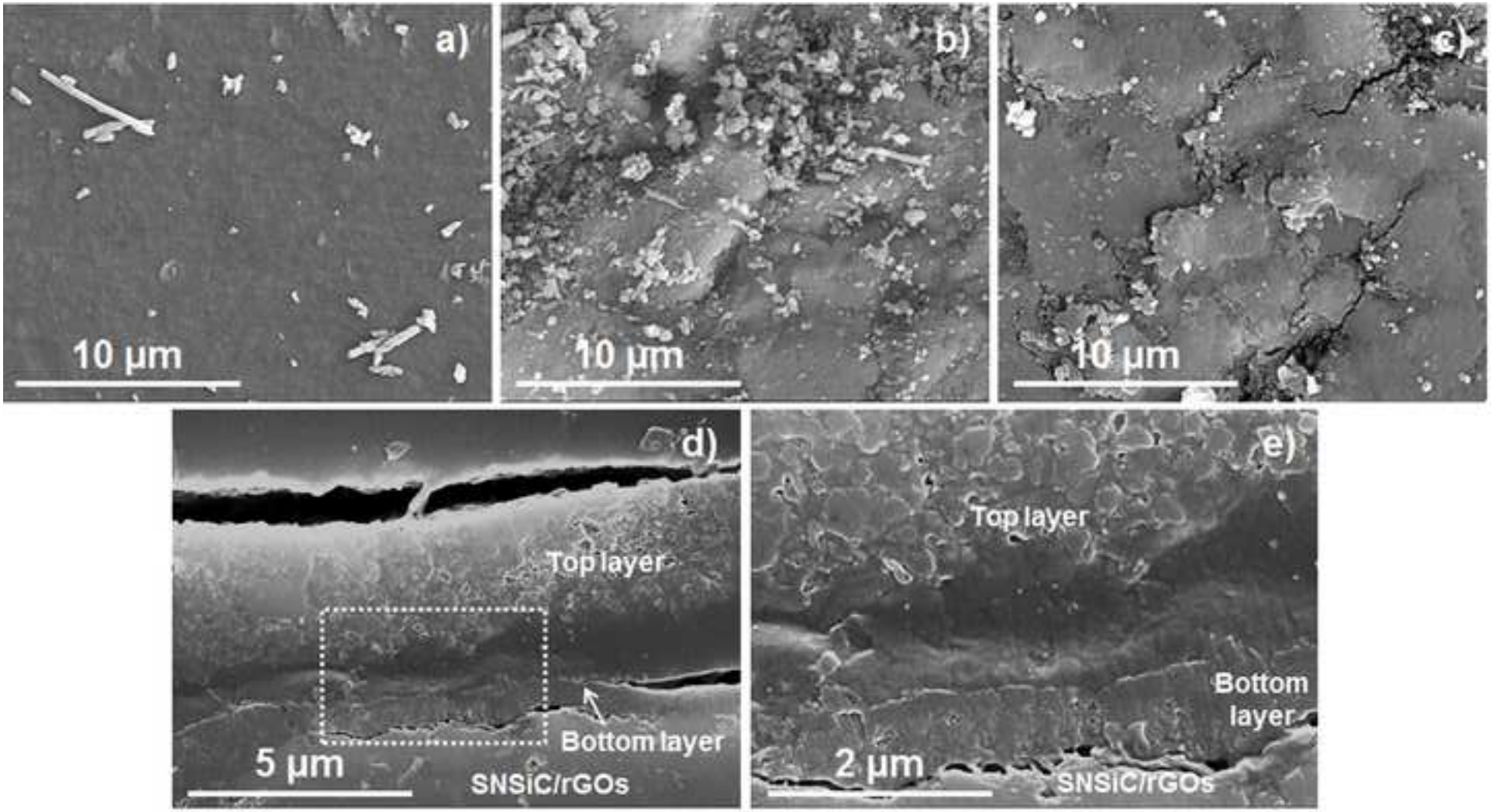

Figure 8

Click here to download high resolution image

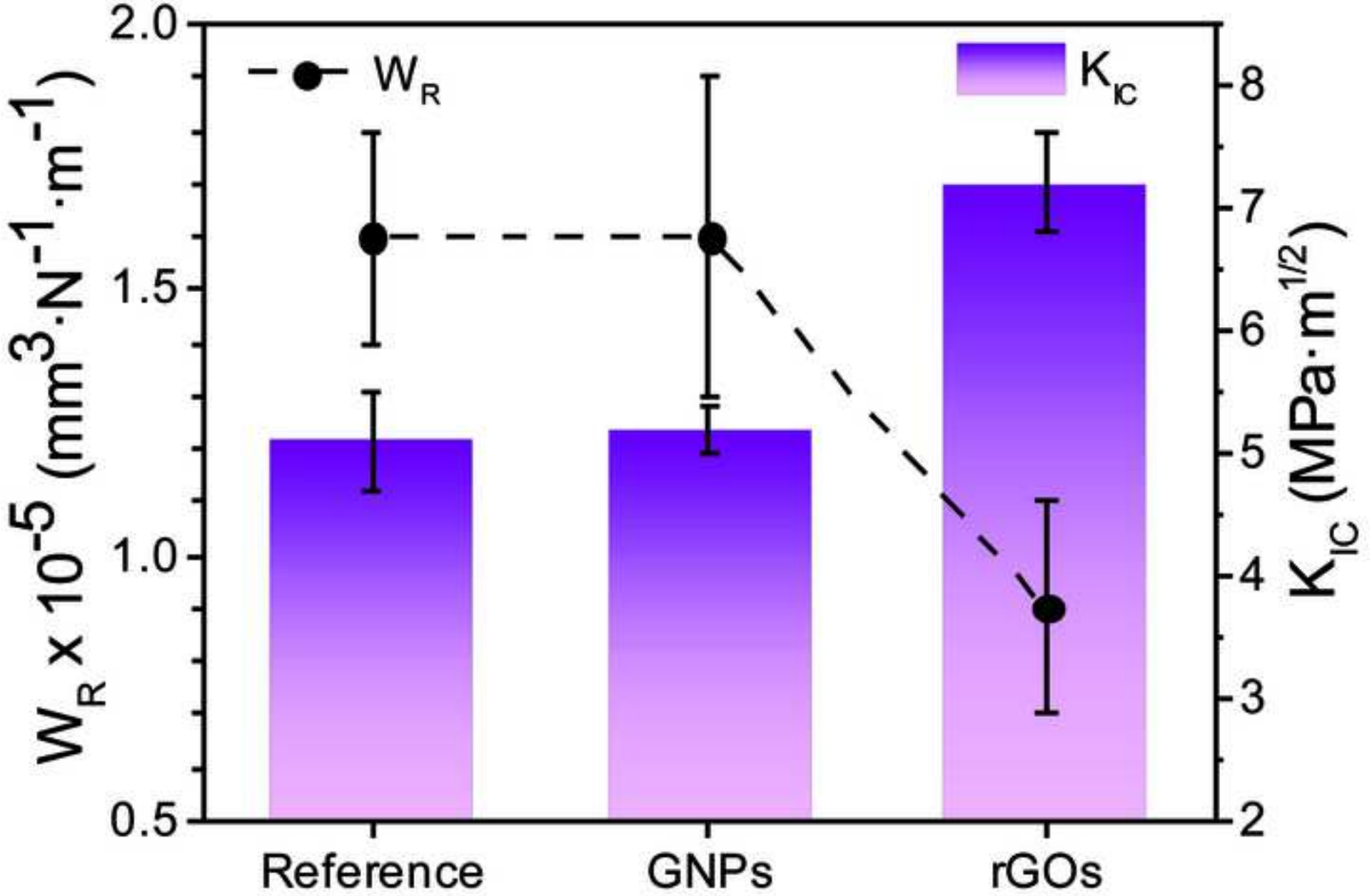

Figure Captions

Figure 1. a) Steady-state friction coefficient (μ_{ss}) and b) wear rates (W_R) of Si_3N_4 ceramics and Si_3N_4/SiC composites as a function of the applied load tested under isooctane lubrication.

Figure 2. SEM images of the cross-section views corresponding to SNSiC/GNPs (a and b) and SNSiC/rGOs (c and d) composites. Images in the left column (a and c) were taken on polished specimens; while those shown in the right column (b and d) are fracture surfaces.

Figure 3. a) Steady-state friction coefficient (μ_{ss}) and b) wear rates (W_R) of SN30-10SiC ceramics (Reference) and SNSiC/GNPs (GNPs) and SNSiC/rGOs (rGOs) composites as a function of the applied load tested under isooctane lubrication.

Figure 4. SEM micrographs of SNSiC (a and c) and SNSiC/rGOs (b and d) tracks after the tests performed under isooctane lubrication at 50 N (a and b) and 180 N (c and d).

Figure 5. W_R versus S_{CM} for SNSiC ceramics and SNSiC/graphene composites as a function of the applied load of tests performed under isooctane lubrication.

Figure 6. a) Average friction coefficient (μ) dynamic evolution considering three valid tests and b) wear rate (W_R) of SN30-10SiC ceramics (Reference) and SNSiC/GNPs (GNPs) and SNSiC/rGOs (rGOs) composites tested under dry conditions.

Figure 7. SEM micrographs of the worn surfaces after the tests performed under dry conditions for: a) the reference material, b) SNSiC/rGOs and c) SNSiC/GNPs composites. d) Image of the cross-section of the tribofilm formed in the SNSiC/rGOs surface and e) high magnification of the area enclosed into the dashed window in d) showing the tribofilm formed by a double layer.

Figure 8. W_R under dry sliding conditions and K_{IC} for SNSiC ceramic and SNSiC/graphene composites.

***Declaration of Interest Statement**

Declaration of interests

☒ The authors declare that they have no known competing financial interests or personal relationships that could have appeared to influence the work reported in this paper.

☐The authors declare the following financial interests/personal relationships which may be considered as potential competing interests: